# Capacitance studies of solar cells based on nanostructured „black" silicon with a passivating GaP layer

© *O.P. Mikhaylov*[1], *A.I. Baranov*[1], *A.A. Maksimova*[1,2], *A.V. Uvarov*[1], *E.A. Vyacheslavova*[1], *A.S. Gudovskikh*[1,2]

[1] Alferov University,
194021 St. Petersburg, Russia
[2] St. Petersburg Electrotechnical University „LETI",
197376 St. Petersburg, Russia
E-mail: oleg.mikhaylov.00@gmail.com

*Received May 6, 2025*
*Revised June 30, 2025*
*Accepted July 9, 2025*

The study investigated heterostructure solar cells based on *p*-Si substrates doped with B, featuring a *b*-Si surface created by dry etching. The *n*-layer consisted of a thin film of wide-bandgap GaP grown by plasma-assisted atomic layer deposition. It was demonstrated that irradiation with a 1 MeV electron beam at a fluence of $5 \cdot 10^{14}\,\mathrm{cm}^{-2}$ reduced the short-circuit current density from 26.3 to 12.2 mA/cm$^2$, and at $1 \cdot 10^{15}\,\mathrm{cm}^{-2}$, it further decreased to 2.8 mA/cm$^2$. According to quantum efficiency spectra and deep-level transient spectroscopy data, no significant degradation of the bulk silicon properties was observed. However, after irradiation, a kink appeared in the current-voltage characteristics, indicating the presence of a parasitic barrier in the structure. This barrier is attributed to the degradation of the metallic contact to *n*-GaP due to irradiation-induced damage.

**Keywords:**gallium phosphide (GaP), black silicon, admittance spectroscopy, deep-level transient spectroscopy (DLTS).

DOI: 10.61011/SC.2025.04.61720.8113

The today's world is switching to renewable energy and this process has intensified since 2020 when the electricity cost grew considerably. Single-junction solar cell (SC) based on the anisotype heterojunction of amorphous hydrogenated and crystalline silicon (*a*-Si:H/*c*-Si) demonstrate the highest potential in terms of capacity and cost benefits [1,2]. However, this technology has nearly reached its maximum theoretical efficiency, and particularly the *n*-type silicon wafer is extremely sensitive to the influence of any particle flux due to radiation-induced defects that are formed even in low orbits in space. Therefore, researchers are making efforts to find approaches to increase energy generation by decreasing optical loss induced by emitter absorption, and to reduce loss at different sunlight incidence angles.

For this purpose, textured surfaces, in particular black silicon (*b*-Si) [3,4] made by a dry etching process followed by emitter deposition, have been extensively studied recently. Recombination at the interface that negatively affects the efficiency is the key factor of work with this technology. Therefore, investigation of textured silicon surface passivation is crucial for design of high-performance heterostructure *b*-Si-based SC. In this study, *b*-Si was fabricated by cryogenic etching of the KDB 1-20 wafer using the „Oxford PlasmaLab System 100 ICP 380". Etching was performed during 380 s at $-150\,^\circ$C to produce a homogeneous array of fibers 1.4 $\mu$m in height. GaP was chosen for fabricating the emitter in this work because the *n*-GaP/*p*-Si heterojunction may be formed by atomic layer deposition, and the *p*-type wafers are reported to be more resistant to space irradiation [5,6]. Capacitance measurements are the most common and effective methods of investigating interface properties to help identify defects affecting the nonradiative recombination.

Heterostructure SCs are studied in this work. Samples were prepared on a boron-doped (resistivity $1-20\,\mathrm{Ohm \cdot cm}$) *p*-Si wafer by wide-band *n*-GaP semiconductor thin layer deposition. Due to a high valence-band discontinuity, the GaP layer shall limit the transport of holes formed in Si, and due to a low conduction-band discontinuity, shall provide effective electron transport across the conduction band boundary. GaP films 50 nm in thickness were deposited by the plasma-assisted atomic layer deposition using the Oxford PlasmaLab System 100 PECVD during 800 cycles at 380 °C with trimethylgallium and phosphine, and additional silane flow. The lower contact was made of aluminum annealed at 700 °C, moreover, annealing facilitated the activation of the silicon mixture in GaP to achieve the *n*-type conductivity. The upper contact was made of silver deposited by vacuum thermal sputtering using the Auto 500 RF Boc Edwards system. Then some samples were irradiated by a 1 MeV electron flux with the fluences of $5 \cdot 10^{14}\,\mathrm{cm}^{-2}$ and $1 \cdot 10^{15}\,\mathrm{cm}^{-2}$. These fluences were chosen with a view to using in low near-Earth orbits. Volt-ampere characteristics and quantum efficiency spectra were measured in the samples before and after irradiation, and the deep level transient spectroscopy (DLTS) was also conducted. This is an effective method to investigate defect levels in semiconductor devices and heterojunctions. The method is based on the capacity relaxation measurement of the space charge region after filling with the bias voltage pulse. Capacity relaxation rate is defined by the carrier emission rate from possible deep

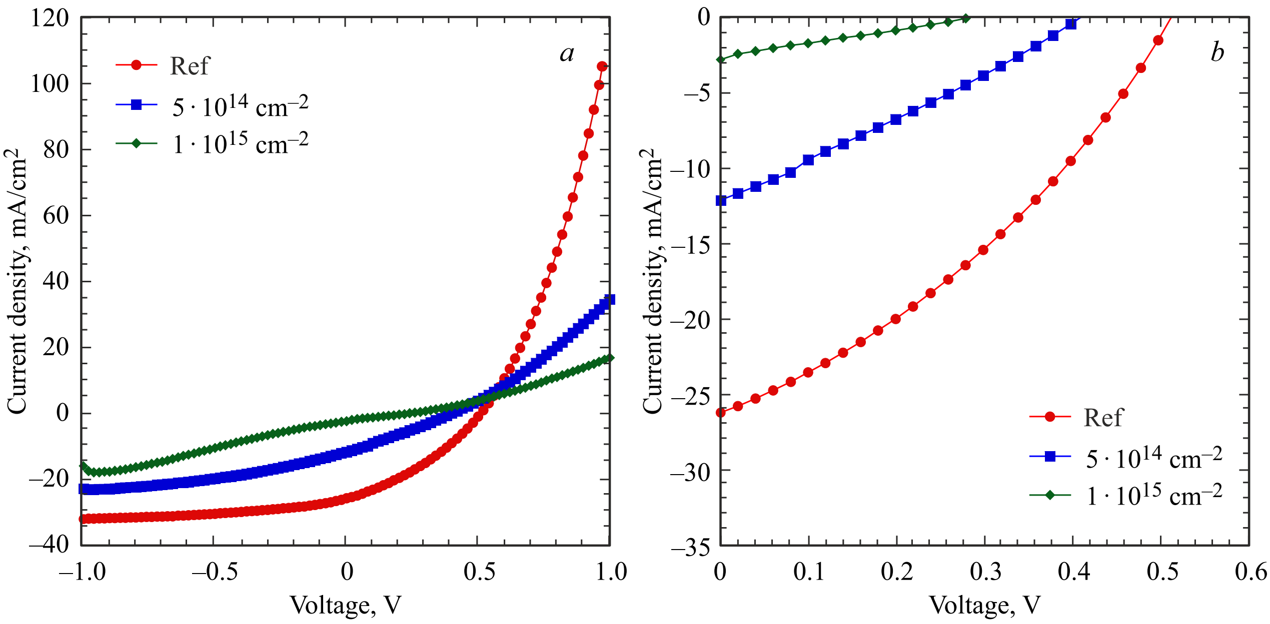


**Figure 1.** Volt-ampere characteristic (*a*) and the 4th quadrant of the volt-ampere characteristic (*b*) of samples irradiated by 1 MeV electrons with the fluences of $5 \cdot 10^{14}\,\mathrm{cm}^{-2}$ and $1 \cdot 10^{15}\,\mathrm{cm}^{-2}$ as well as initial samples.

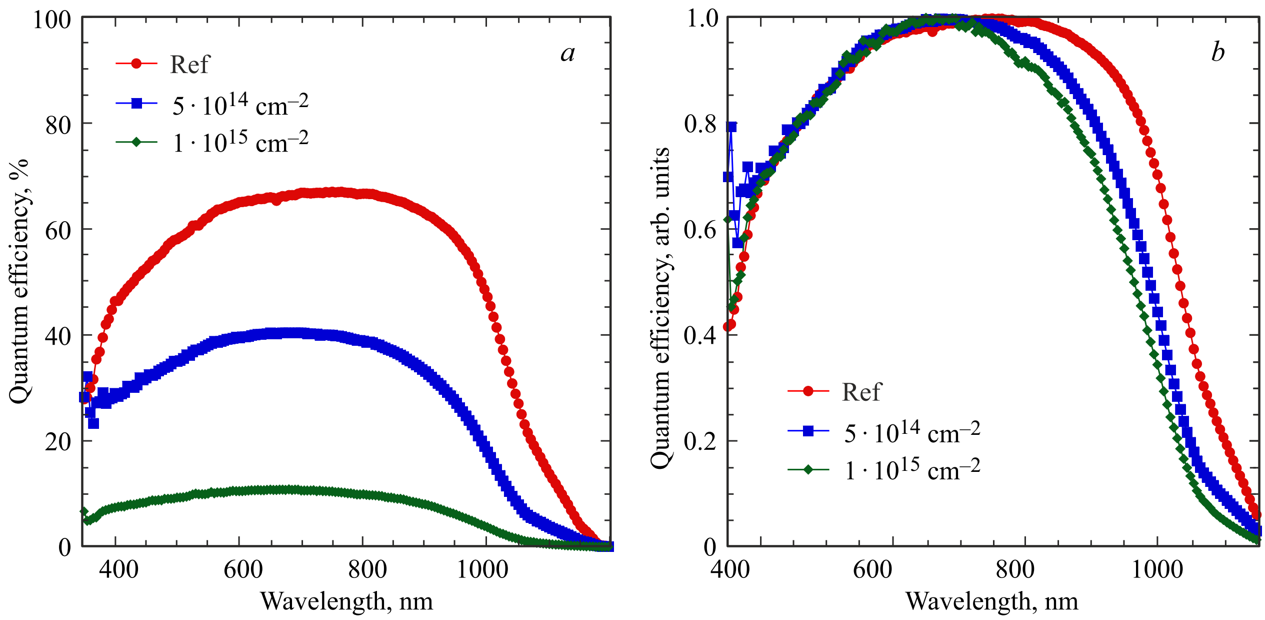


**Figure 2.** Measured (*a*) and normalized (*b*) spectra of the external quantum efficiency of the *n*-GaP/*p*-Si test samples.

levels in the semiconductor band gap that in turn depends on temperature. Deep level transient spectroscopy was performed using the Boonton-7200B capacitance-bridge automated system in the temperature range of 78–300 K in the Janis CCS-400H/204 helium cryostat. The system is used to apply bias voltage with various amplitudes, all measurements were performed in LabView.

Figure 1 shows VAC of the *n*-GaP/*p*-*b*-Si samples before and after exposure to electrons with the above-mentioned energy and fluences in AM1.5G light at 25 °C.

When reviewing Figure 1, *a* and *b*, correlation of the volt-ampere characteristic depending on the irradiation fluence may be noted. When the fluence is $5 \cdot 10^{14}\,\mathrm{cm}^{-2}$, short-circuit current decreases by 54 %, to 12.2 mA/cm$^2$ with respect to initial 26.3 mA/cm$^2$. When the fluence is $1 \cdot 10^{15}\,\mathrm{cm}^{-2}$, short-circuit current decreases by 89 %, to 2.8 mA/cm$^2$. There is also no-load voltage drop from initial 520 mV to 420 mV with the fluence of $5 \cdot 10^{14}\,\mathrm{cm}^{-2}$ and to 280 mV with the fluence of $1 \cdot 10^{15}\,\mathrm{cm}^{-2}$. When looking at the shape of volt-ampere curves in Figure 1, *b*, it is obvious that the filling factor decreases because the VAC of the irradiated samples deviates from the exponential behavior. This becomes especially apparent in Figure 1, *a* where a kink on the VAC curve occurs, in particular, at $1 \cdot 10^{15}\,\text{cm}^{-2}$. VAC degradation may be induced by several reasons: degradation of the GaP layer properties, occurrence of recombination centers at the silver and GaP interface, at the *n*-GaP/*p*-*b*-Si heterojunction interface, formation of centers within the Si wafer.

Short-circuit current is affected by the quantum efficiency spectrum measured at 0 V in the wavelength range from 350 nm to 1200 nm (Figure 2).

Review of the resulting curve shows virtually uniform drop of the external quantum efficiency (EQE) in the entire wavelength range for the irradiated samples: by a factor of $\sim 2$ with respect to the initial value for the fluence of $5 \cdot 10^{14}\,\text{cm}^{-2}$, and by a factor of 7 for the fluence of $1 \cdot 10^{15}\,\text{cm}^{-2}$. However, when the quantum efficiency spectra are normalized, a minor change of the curves can be seen only in the long-wavelength region from 800 nm to 1200 nm, while in the short-wavelength region the curves almost coincide. Such uniform decrease in EQE for the entire range may indicate that the irradiation probably degrades the structure properties in general irrespective of the wavelength, which may be observed in case of degradation of the GaP layer and the GaP layer-silver interface, and occurrence of spurious leakage currents. In other words, formation of nonradiative recombination centers near the Si surface or of additional surface states at the GaP/*p*-Si interface would cause considerable EQE drop in the short-wavelength region, where high energy photons are absorbed effectively. On the other hand, formation of a great amount of defects within Si would cause nonuniform drop in the long-wavelength region due to reduced lifetime in the wafer. Such EQE drop was observed in the previous studies of samples based on the *p*-*a*-Si/*i*-*a*-Si/*n*-*c*-Si [7] anisotype heterojunction and is typical of *n*-Si. Thus, the VAC and EQE behavior suggests that electron irradiation doesn't induce any significant degradation of properties within the Si wafer and in the near-surface region.

This fact was verified using DLTS to detect defects within silicon. Figure 3 shows the DLTS spectra measured at the following parameters for different time windows.

Review of the curves suggested that no increase in the concentration of defects was observed after irradiation. Defects with activation energies of $E1 = 0.18\,\text{eV}$ and $E2 = 0.35\,\text{eV}$ were also found, concentration of these defects was not higher than $10^{12}\,\text{cm}^{-3}$. As a result, no significant differences in the bulk properties of Si are observed after irradiation, therefore, degradation of the VAC behavior is induced by imperfection of the metal-to-*n*-GaP contact and degradation of the layer properties after irradiation. Therefore, future efforts will be focused on optimizing the silver and *n*-GaP layers.

Thus, the study investigated the effect of electron irradiation on the photovoltaic properties of *n*-GaP/*p*-S

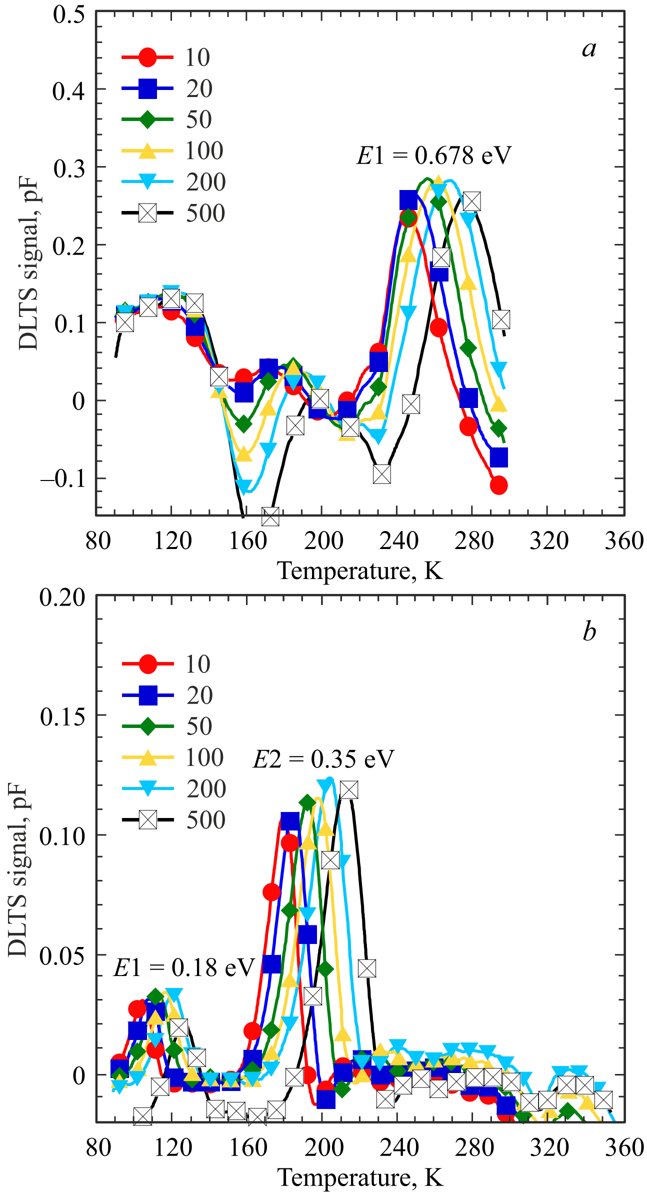


**Figure 3.** DLTS spectrum diagram for the initial sample (*a*) and the sample irradiated by 1 MeV electrons with the fluence of $5 \cdot 10^{14}\text{cm}^{-2}$ (*b*). The measurements were performed at $V_{\text{init}} = -2\,\text{V}$, $V_{\text{pulse}} = 2\,\text{V}$.

photoconverter heterostructures formed on the black silicon surface. The initial sample had $J_{\text{shc}} = 26.3\,\text{mA/cm}^2$ and $V_{\text{id}} = 520\,\text{mV}$, after irradiation with $5 \cdot 10^{14}\,\text{cm}^{-2}$ the parameters decreased to $12.2\,\text{mA/cm}^2$ and 420 mV, respectively, and with $1 \cdot 10^{15}\,\text{cm}^{-2}$ the parameters decreased to $2.8\,\text{mA/cm}^2$ an 280 mV. According to the quantum efficiency spectra undergoing monotonic drop with the increase in the fluence at all wavelengths and the DLTS spectra measured deep in the wafer, no significant degradation of properties occurs within Si. On the contrary, a kink occurs in the VAC after irradiation indicating that there is a spurious barrier in the structure caused by the imperfection of the metal-to-*n*-GaP contact due to the degradation of its properties after irradiation.

### Funding

The study was performed within project No. 24-79-10275 of the Russian Science Foundation https://rscf.ru/prjcard_int?24-79-10275

### Conflict of interest

The authors declare no conflict of interest.

## References

[1] Y. Liu, Y. Li, Y. Wu, G. Yang, L. Mazzarella, P. Procel-Moya, A. Tamboli, K. Weber, M. Boccard, O. Isabella, X. Yang, B. Sun. Mater. Sci. Eng. R: Reports, **142**, 100579 (2020). DOI: 10.1016/j.mser.2020.100579

[2] S. De Wolf, A. Descoeudres, Z.C. Holman, C. Ballif. Green, **2**, 7 (2012). DOI: 10.1515/green-2011-0018

[3] E.A. Vyacheslavova, A.V. Uvarov, A.A. Maksimova, A.I. Baranov, A.S. Gudovskikh. St. Petersburg State Polytechnical University J. Phys. and Math., **16** (3.1), 434 (2023). DOI: https://doi.org/10.18721/JPM.163.179

[4] M. Mews, C. Leendertz, M. Algasinger, S. Koynov, L. Korte. Phys. Status Solidi: Rapid Res. Lett., **8** (10), 831 (2014). DOI: 10.1002/pssr.201409327

[5] M. Yamaguchi, K.-H. Lee, K. Araki, N. Kojima, Y. Okuno, M. Imaizumi. Progr. Photovolt.: Res. Appl., **29** (1), 98 (2021). DOI: https://doi.org/10.1002/pip.3346

[6] Sh.B. Utamuradova, E.I. Terukov, O.K. Ataboev, I.E. Panaiotti, R.R. Kabulov, A.V. Troshin. Nucl. Instrum. Meth. Phys. Res. B, **560**, 165630 (2025). https://doi.org/10.1016/j.nimb.2025.165630

[7] O.P. Mikhaylov, A.I. Baranov, A.V. Uvarov, A.A. Maksimova, E.A. Vyacheslavova, A.S. Gudovskikh, M.Z. Shvarts, E.I. Terukov. St. Petersburg State Polytechnical University J. Phys. and Math., **17** (3.2), 251 (2024). DOI: https://doi.org/10.18721/JPM.173.250

*Translated by E.Ilinskaya*